

Efficient Coupling From Dielectric to Hybrid Plasmonic Waveguide Using Curved Taper

Virendra Patel^{ID}, *Student Member, IEEE*, Prateeksha Sharma^{ID}, *Student Member, IEEE*,
and V. Dinesh Kumar^{ID}, *Member, IEEE*

Abstract—This is the first report on the investigation of a realistic 3D hybrid metal–insulator–silicon–insulator–metal (MISIM) plasmonic tapered coupler, which efficiently couples light from dielectric to multilayer (MISIM) hybrid plasmonic waveguide. The structure is designed to achieve high transmission efficiency and to suppress the reflection losses. The proposed coupler exhibits a maximum transmittance up to **99%** and a minimum mode propagation loss of $0.07 \text{ dB}/\mu\text{m}$ at $1.55\text{-}\mu\text{m}$ wavelength. The structure is designed using an ultra-short curved taper length of $1.5 \mu\text{m}$, and it occupies a footprint area of $5.94 \mu\text{m}^2$, which is several folds reduced compared to the previous reports. This investigation provides a basis for the future nanoscale photonics of practical applications.

Index Terms—Couplers, hybrid plasmonics waveguide, plasmonic coupler, plasmonic waveguides, silicon photonics.

I. INTRODUCTION

HIGH speed optical couplers are important elements for designing plasmonic integrated circuits, as it efficiently couples light from micron size dielectric structures to nanometer size plasmonic structures on the same platform [1]–[15]. So far several connectors and couplers are studied for integration of dielectric and plasmonics structures such as direct, grating, evanescent, end-fire and prism couplers etc. Direct coupler offers huge mismatch losses, resulting in poor efficiency [11]. Grating coupler increases system complexity resulting tedious fabrication [7], [8]. End-fire coupling requires proper alignment, which is again a challenging task at nanometer scale and prism couplers are bulky in size [12]. Taper coupler seems a viable solution, where modes change gradually with taper length [11]. But for achieving high efficiency a larger length coupler is needed, which increases footprint area of system. Also longer metal track may enhance ohmic loss.

Hence, in this letter, we propose a novel 3D curve shaped MISIM (Metal–Insulator–Silicon–Insulator–Metal) hybrid plasmonic taper coupler for efficient light coupling from dielectric to multilayer hybrid plasmonic (MISIM) waveguide for the first time. MISIM hybrid plasmonic coupler is compact in size, offers high efficiency and least radiation losses over three

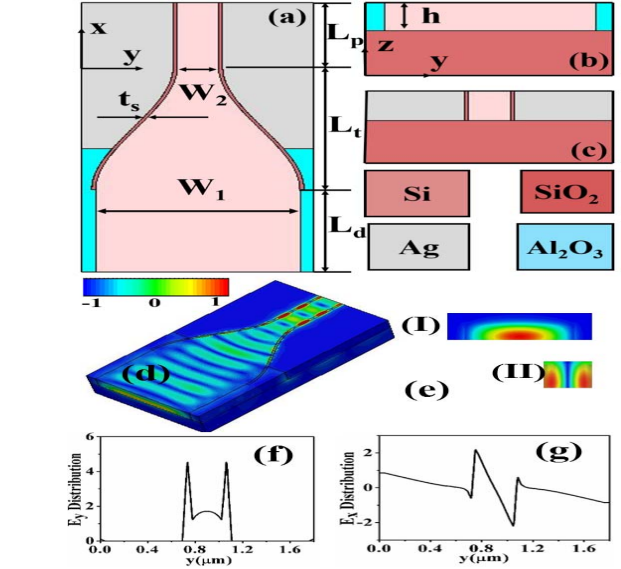


Fig. 1. (a) Top view of the curve tapered structure, Cross section view of (b) Input dielectric waveguide (c) Output MISIM plasmonic waveguide, (d) Propagation of light from dielectric to plasmonic waveguide (e) Mode profile in (I) dielectric waveguide and (II) plasmonic waveguide (f) E_y , (g) E_x distribution in plasmonics waveguide at $1.55 \mu\text{m}$ wavelength.

layer hybrid plasmonic coupler. Moreover, they are practically feasible unlike the purely plasmonic couplers.

The transmission and loss characteristics of proposed coupler are calculated at $1.55 \mu\text{m}$ operating wavelength using rigorous parametric variations. The performance of the proposed coupler is better than previously reported couplers in several aspects such as transmission & loss characteristics, design & fabrication complexities, size miniaturization etc. [1]–[15]. In order to set the benchmark, performance comparison has also been given at the end, between linear and curved taper transition from dielectric to hybrid plasmonic waveguides. This study may be useful in designing practical hybrid plasmonic integrated circuits for the Nanophotonic application.

II. MODELING AND SIMULATION METHOD

Schematic of the proposed MISIM (Ag-SiO₂-Si-SiO₂-Ag) curved tapered coupler along with multilayer hybrid plasmonic and input dielectric waveguides is shown in Fig. 1(a)–(c). The permittivity of silver (Ag) is defined by Drude model such as, $\epsilon_m = \epsilon_\infty - \frac{\omega_p^2}{\omega^2 + j\omega\Gamma}$. Here $\epsilon_\infty = 1$ is dielectric constant at the infinite angular frequency, $\omega_p = 1.39 \times 10^{16} \text{ rad/s}$ is the bulk plasma frequency and $\Gamma = 3.08 \times 10^{13} \text{ s}^{-1}$

Manuscript received July 16, 2018; revised November 22, 2018; accepted January 16, 2019. Date of publication January 23, 2019; date of current version February 5, 2019. (Corresponding author: Virendra Patel.)

The authors are with the Discipline of Electronics and Communications, Indian Institute of Information Technology, Design and Manufacturing, Jabalpur 482005, India (e-mail: viru.rgh@gmail.com).

Color versions of one or more of the figures in this letter are available online at <http://ieeexplore.ieee.org>.

Digital Object Identifier 10.1109/LPT.2019.2894368

is the damping frequency of oscillation [16]. At $1.55 \mu\text{m}$ operating wavelength the permittivity of silver is calculated as; $\epsilon_\infty = -129 + 3.3i$. Refractive indices for SiO_2 , Si, and Al_2O_3 are $n_{\text{SiO}_2} = 1.44$, $n_{\text{Si}} = 3.5$ and $n_{\text{Al}_2\text{O}_3} = 1.73$ respectively [17], [18]. Silica and air are used for substrate and cladding respectively.

Light is coupled from dielectric waveguide to MISIM hybrid plasmonic waveguide with the help of MISIM curve tapered hybrid plasmonic coupler, as shown in Fig. 1(a). Input dielectric waveguide is designed by sandwiching silicon layer by Al_2O_3 layers. Al_2O_3 is basically used to reduce the mode transition losses [9]. Width of Si layer in the input dielectric slab is defined as; $W_1 = 1.50 \mu\text{m}$. Widths of Si and silica are set as; $W_2 = 0.30 \mu\text{m}$ and $t_s = 0.03 \mu\text{m}$ respectively in MISIM hybrid plasmonic waveguide, as shown in Fig. 1(a)-(c). Parameters $L_d = 1.0 \mu\text{m}$, $L_t = 1.5 \mu\text{m}$, $L_p = 0.8 \mu\text{m}$ designate the lengths of dielectric waveguide, tapered region, and MISIM waveguide respectively, as shown in Fig. 1(a)-(c). The thickness ‘h’ of the waveguide is taken as $0.30 \mu\text{m}$. The curve of the tapered coupler is defined in terms of cosine function as: $(W_1 - W_2) * (1 - \cos(\pi * x / L_t) / 4)$ [3].

All simulations are performed using frequency domain solver of CST microwave studio suite, which is a comprehensive 3D electromagnetic tool for design and analysis. Perfect matched layer boundary conditions are applied to all boundaries of the simulation domain and refined meshing of 25 tetrahedrons per wavelength are used for accurate results.

Before the present computation, results in [6]–[8] are verified using this software which validates our simulation procedure. The proposed coupler is a realistic structure and can be fabricated by standard semiconductor fabrication methods. Different layers can be deposited by PECVD (Plasma enhanced chemical vapor deposition), oxidation, and metallization processes. Subsequently waveguide patterning to typical nanometer dimensions may be done using E-beam lithography. Unwanted metal and dielectric layers may be etched out using reactive ion etching process [17].

III. RESULTS AND DISCUSSION

To couple light in MISIM plasmonic waveguide, firstly light is launched into the dielectric waveguide, as shown in Fig. 1(d). Optical power is well-confined in the dielectric waveguide because of TIR (total internal reflection). Next, light passes through the curve tapered hybrid plasmonic coupler, and this transition region with cosine profile gradually transforms the dielectric mode in Al_2O_3 -Si- Al_2O_3 waveguide into hybrid plasmonic mode in narrow Ag-SiO₂-Si-SiO₂-Ag multilayer hybrid plasmonic waveguide resulting in efficient light injection. For illustration, the absolute electric field distribution is shown at input and output sections of the proposed tapered coupler in Fig 1(e). At the input waveguide (Al_2O_3 -Si- Al_2O_3) light propagates through high index medium i.e. Si due to TIR and modes are purely dielectric modes, as shown in Fig. 1(e)I. Effective refractive index $\text{Re}(N_{\text{eff}})$ decreases with reduced Si layer width, which results in slightly reduced field concentration in this layer. Thus dielectric mode becomes slightly weak. Evidently the

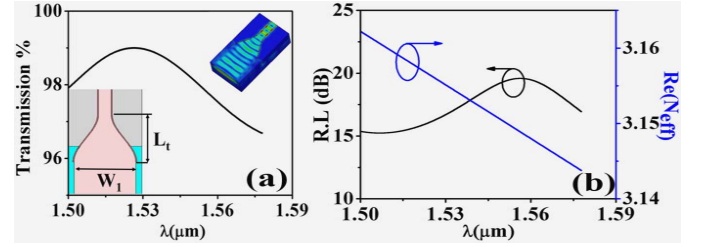


Fig. 2. Simulated results of curved taper coupler for optimized parameters ($W_1 = 1.50 \mu\text{m}$, $W_2 = 0.30 \mu\text{m}$, $t_s = 0.03 \mu\text{m}$, $L_d = 1.0 \mu\text{m}$, $L_t = 1.5 \mu\text{m}$ and $L_p = 0.8 \mu\text{m}$). (a) Transmission from dielectric to plasmonics, (b) Return loss in dB and $\text{Re}(N_{\text{eff}})$ in wavelength band of $1.50 \mu\text{m}$ to $1.58 \mu\text{m}$.

TABLE I
EFFICIENCY (η) COMPARISON AGAINST PREVIOUS LITERATURE

References	[6]	[7], [11], [15]	[8]	[12]	[13]	[14]
$\eta(\%)$	40	70	96	35	33	38

field concentration in Ag-SiO₂ region gets increased. The modes evolve into hybrid plasmonic modes with the gradual decrement in the Si layer width, as shown in Fig. 1(e)II. In this case, mostly power is guided through thin silica layer due to coupling of plasmonic and dielectric modes. These coupled modes are called hybrid plasmonic modes. 2D E-field distributions are also calculated at the output end. A line is drawn horizontally at the center, connecting both metal films. It is visible from (E_y) and (E_x) plots shown in Fig. 1(f) and (g) respectively that most share of energy gets confined in thin silica layers of MISIM hybrid plasmonic waveguide. Thus the tapered coupling helps in reducing return losses and curvature minimizes radiation losses while transforming modes gradually. Moreover, the proposed hybrid plasmonic coupler offers less ohmic losses unlike the purely plasmonic couplers, hence coupling efficiency gets increased.

Parameters of proposed MISIM curved tapered coupler are already defined in section II, which are optimized by several parametric variations for optimal performance. Performance of the proposed structure can be defined by two important parameters, first is mode propagation length i.e. ‘ L_{prop} ’ and other is mode losses (M.L.). Mode propagation length is defined as; $L_{\text{prop}} = \lambda_0 / 4\pi (\text{Imag}(N_{\text{eff}}))$, where λ_0 is the operating wavelength and $\text{Imag}(N_{\text{eff}})$ is the imaginary part of effective refractive indices, which can be calculated as, $\text{Imag}(N_{\text{eff}}) = \alpha / k_0$, here α and k_0 are attenuation constant and wave number respectively [19]. Loss calculation of the proposed structure is done by: $M.L. = -10 \log(1/e) / L_{\text{prop}} \approx 4.343 / L_{\text{prop}}$ [20].

Propagation length and loss are found as; $58 \mu\text{m}$ & $0.07 \text{ dB}/\mu\text{m}$ respectively for the optimized parameters. Transmission and return loss characteristics are also plotted for the proposed coupler in a wavelength range of $1.50 \mu\text{m}$ to $1.58 \mu\text{m}$, as shown in Fig. 2(a)-(b). It is observed that the coupler shows upto 99% efficiency in the given band for the optimized parameters, which is much superior to previous reports in literature. Efficiency of proposed curved taper coupler is compared against previous reported coupler in Table I. Fig. 2(b) shows return loss ($RL = 10 \log_{10}(P_{\text{out}}/P_{\text{in}})$) and $\text{Re}(N_{\text{eff}})$ in the wavelength range $1.50 \mu\text{m}$ to $1.58 \mu\text{m}$.

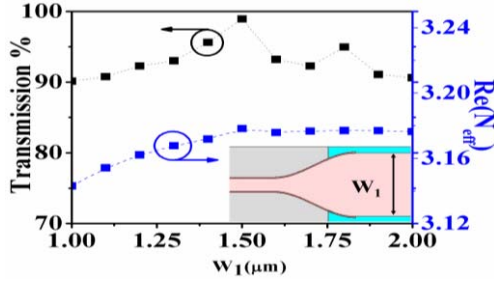


Fig. 3. Transmission and real effective mode index ($Re(N_{eff})$) for different widths of silicon 1.00 μm -2.00 μm at 1.55 μm .

RL up to 20 dB has been observed in the given band. $Re(N_{eff})$ exhibits the dispersion properties, which is defined as $Re(N_{eff}) = \beta/k_0$, where β is phase constant.

It is observed from Fig. 2(b) that $Re(N_{eff})$ is dependent on wavelength and it decreases linearly with increasing wavelength. The sidewall of the real device may have large roughness resulting in propagation losses. To ensure the practical realization of the proposed coupler, the effects of surface roughness and scattering losses at metal dielectric interfaces are also examined by numerical simulation, which gives an insight into performance degradation of the real structure. Height (Y-dimension) is varied randomly as t_m , $t_m \pm 0.003 \mu\text{m}$, $t_m \pm 0.025 \mu\text{m}$, where t_m is the metal slab thickness in Y-direction. and width (X-dimension) is varied randomly as 0.001 μm , 0.002 μm , 0.003 μm , 0.004 μm , 0.005 μm . It is found that the transmission drops from 99% for the smooth surface to 77% for the maximum roughness. It reveals that the proposed coupler is sensitive to such fabrication imperfection but its performance is within the tolerance limit (21%). Further, the performance of coupler is investigated for various geometric features such as: (A) Input dielectric waveguide width (W_1), (B) Width of silica film of curved taper coupler (t_s), and (C) Taper length (L_t), which are discussed in the further analysis.

A. Dielectric Waveguide Width Variation (W_1)

Dielectric to MISIM hybrid plasmonic coupler has been analyzed for different silicon widths ($W_1 = 1.0$ -2.0 μm) at 1.55 μm operating wavelength, as shown in Fig. 3. Dielectric waveguide width has a greater impact on the transmission efficiency. Initially transmission increases with W_1 due to increased mode matching between dielectric and hybrid plasmonic waveguides. But after a certain width, it decreases on further increase in W_1 , reason may be poor mode matching due to increased abruptness in structure. Maximum transmission of 99 % has been observed at $W_1 = 1.50 \mu\text{m}$. $Re(N_{eff})$ increases with increasing W_1 , as shown in Fig. 3, as dielectric modes become more dominant.

B. Silica Film Width Variation (t_s)

Next, coupler analysis is done by varying silica film width (t_s), as shown in Fig. 4(a). Transmission efficiency increases first and then reduces with increase in t_s . At the low value of t_s , the proposed coupler waveguide acts as a standard plasmonic waveguide, hence suffers from severe ohmic losses,

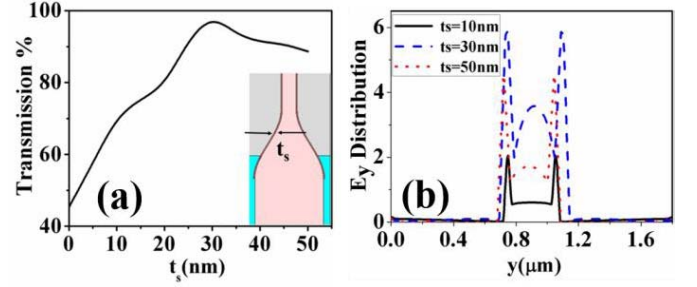


Fig. 4. (a) Transmission efficiency of coupler with respect to silica thickness t_s (b) (E_y) field distribution at the output plasmonic end for different silica thickness of 10 nm, 30 nm & 50 nm.

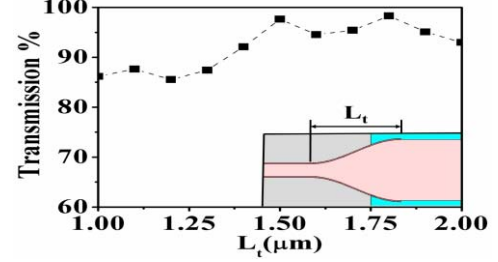


Fig. 5. Transmission with respect to taper length ($L_t = 1.0 \mu\text{m}$ -2.0 μm).

resulting in reduced transmission efficiency. On the other hand, at higher values of t_s , $Re(N_{eff})$ reduces due to the low refractive index of silica, hence energy is less confined in coupler waveguide, this again results in reduced transmission efficiency. Maximum transmission of 99% has been observed for $t_s = 0.03 \mu\text{m}$, at the balancing condition, when hybrid modes are excited optimally [4]. Next, E_y field distribution is also plotted at different spacer thicknesses ($t_s = 10, 30, 50 \text{ nm}$) as shown in Fig. 4(b). Plasmonic modes are excited at the low value of t_s (i.e. 10 nm) and mostly energy is confined at metal-dielectric interface and less in spacer layers. At high value of t_s (i.e. 50 nm), there will be less coupling between dielectric and plasmonic modes causing less energy confinement again in the spacer layers. Perfect coupling between dielectric and plasmonic modes occur at the intermediate thickness (i.e. $t_s = 30 \text{ nm}$), allowing the proper excitation of hybrid plasmonic modes. At this, high peak of E-field in both spacer layers are observed, as shown in Fig. 4(b).

C. Taper Length of Coupler (L_t)

Next, transmission efficiency is highly dependent on taper length, as again dispersion properties vary with it. The transmission has been calculated for $L_t = 1.0 \mu\text{m}$ to 2.0 μm at 1.55 μm wavelength, as shown in Fig. 5. At the low value of L_t , there may be radiation losses, which results in poor transmission. Transmission increases on increasing L_t , as it overcomes from radiation losses, and it reaches up to 99% at 1.5 μm taper length. For the taper lengths (1.5 μm and 1.80 μm), the incident light falling on curve taper are in phase, hence offers maximum coupling efficiency. However, transmission reduces further increasing L_t , the reason being increased track length, which causes severe ohmic losses.

D. Analysis of Dielectric to Dielectric Coupler (DtD)

Further, Dielectric to dielectric (DtD) coupler has been designed and analyzed for better understanding of performance

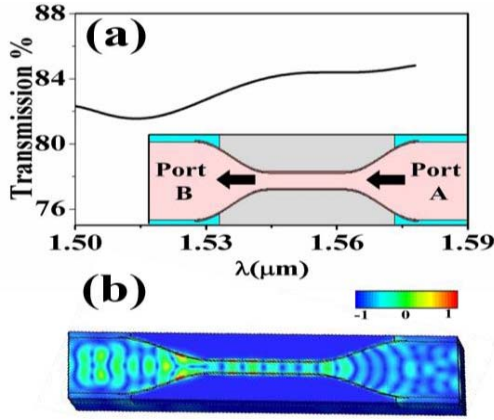


Fig. 6. (a) Transmission for dielectric to dielectric (DtD) curved taper coupler with optimized parameters as in section II. (b) 3D E-field view of DtD coupler.

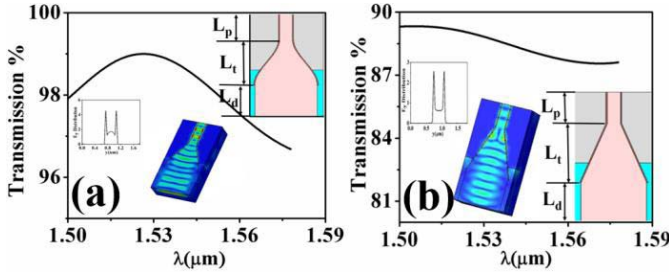


Fig. 7. Comparison of the result (a) curve tapered coupler (b) MISIM with linear taper respectively. For both structures, the parameters are as same as mentioned in section II.

as shown in Fig. 6. Two dielectric to plasmonic couplers are connected back to back for designing the dielectric to dielectric coupler, as shown in Fig. 6(a). Firstly dielectric modes couple in MISIM plasmonic waveguide and then decouples into dielectric waveguide through MISIM curve tapered coupler. It occupies a very compact footprint area of $11.88 \mu\text{m}^2$. Highest transmission efficiency of 84% has been observed, which shows that proposed MISIM curve tapered coupler is very efficient even as a coupling-decoupling structure. 3D E-field distribution of the proposed DtD coupler is also shown in Fig. 6(b).

E. Comparative Analysis

In order to set a benchmark, we compare the performance of our proposed curve tapered MISIM coupler against the linear tapered MISIM coupler on the same footprint area, as shown in Fig. 7(a)-(b). It is found that the MISIM hybrid plasmonic coupler with curve taper offers higher transmission efficiency up to 99%, as shown in Fig. 7(a). Comparatively, the coupler with linear taper has inferior transmission up to 87%, as shown in Fig. 7(b). In curve tapered coupler, the smooth transition from dielectric to MISIM plasmonic waveguide, mitigates the radiation losses and hence improves the transmission efficiency unlike the tapered coupler without curve.

IV. CONCLUSION

In this letter, a realistic curve tapered coupler, based on hybrid MISIM plasmonic waveguide has been proposed and investigated for the first time at $1.55 \mu\text{m}$ wavelength. Efficient

coupling of light is achieved from dielectric to MISIM hybrid plasmonic waveguide. The proposed coupler offers transmission, mode propagation loss and propagation length of 99%, $0.07 \text{ dB}/\mu\text{m}$ and $58 \mu\text{m}$ respectively, which are superior to previous reports. Further the proposed curve tapered coupler has been compared against linear tapered coupler with same set of parameters, which establishes its superiority. Finally a DtD coupler is obtained by combining two curve tapered couplers and its performance is evaluated. This study may permit replacement of previous reported couplers.

REFERENCES

- [1] H. J. Lim and M. S. Kwon, "Efficient coupling between photonic and dielectric-loaded surface plasmon polariton waveguides with the same core material," *IEEE Photon. J.*, vol. 6, no. 3, Jun. 2014, Art. no. 4800809.
- [2] L. Chen *et al.*, "A silicon-based 3-D hybrid long-range plasmonic waveguide for nanophotonic integration," *J. Lightw. Technol.*, vol. 30, no. 1, pp. 163–168, Jan. 1, 2012.
- [3] P. Sharma and V. D. Kumar, "Investigation of multilayer planar hybrid plasmonic waveguide and bends," *Electron. Lett.*, vol. 52, no. 9, pp. 732–734, Apr. 2016.
- [4] P. Sharma and V. D. Kumar, "Hybrid insulator metal insulator planar plasmonic waveguide-based components," *IEEE Photon. Technol. Lett.*, vol. 29, no. 16, pp. 1360–1363, Aug. 15, 2017.
- [5] L. Chen, T. Zhang, X. Li, and W. Huang, "Novel hybrid plasmonic waveguide consisting of two identical dielectric nanowires symmetrically placed on each side of a thin metal film," *Opt. Express*, vol. 20, no. 18, pp. 20535–20544, 2012.
- [6] R. Thomas, Z. Ikonik, and R. W. Kelsall, "Silicon based plasmonic coupler," *Opt. Express*, vol. 20, no. 19, pp. 21520–21531, 2012.
- [7] P. Ginzburg, D. Arbel, and M. Orenstein, "Efficient coupling of nano-plasmonics to micro-photonic circuitry," in *Conf. Lasers Electro-Opt./Quantum Electron. Laser Sci. Photon. Appl. Syst. Technol. (CD) Tech. Dig.*, May 2005, pp. 1482–1484, Paper CWN5.
- [8] Y. Liu, Y. Lai, and K. Chang, "Plasmonic coupler for silicon-based micro-slabs to plasmonic nano-gap waveguide mode conversion enhancement," *J. Lightw. Technol.*, vol. 31, no. 11, pp. 1708–1712, Jun. 1, 2013.
- [9] C. T. Chen *et al.*, "Design of highly efficient hybrid Si-Au taper for dielectric strip waveguide to plasmonic slot waveguide mode converter," *J. Lightw. Technol.*, vol. 33, no. 2, pp. 535–540, Jan. 15, 2015.
- [10] L. Chen, X. Li, and D. Gao, "An efficient directional coupling from dielectric waveguide to hybrid long-range plasmonic waveguide on a silicon platform," *Appl. Phys. B, Lasers Opt.*, vol. 111, no. 1, pp. 15–19, Apr. 2013.
- [11] Y. Song, J. Wang, Q. Li, M. Yan, and M. Qiu, "Broadband coupler between silicon waveguide and hybrid plasmonic waveguide," *Opt. Express*, vol. 18, no. 12, pp. 13173–13179, Jun. 2010.
- [12] J. Tian, S. Yu, W. Yan, and M. Qiu, "Broadband high-efficiency surface-plasmon-polariton coupler with silicon-metal interface," *Appl. Phys. Lett.*, vol. 95, no. 1, p. 013504, Jul. 2009.
- [13] Z. Han, A. Y. Elezzabi, and V. Van, "Experimental realization of subwavelength plasmonic slot waveguides on a silicon platform," *Opt. Lett.*, vol. 35, no. 4, pp. 502–504, Feb. 2010.
- [14] S. Sederberg, V. Van, and A. Y. Elezzabi, "Monolithic integration of plasmonic waveguides into a complimentary metal-oxide-semiconductor-and photonic-compatible platform," *Appl. Phys. Lett.*, vol. 96, no. 12, p. 121101, Mar. 2010.
- [15] P. Ginzburg, D. Arbel, and M. Orenstein, "Gap plasmon polariton structure for very efficient microscale-to-nanoscale interfacing," *Opt. Lett.*, vol. 31, no. 22, pp. 3288–3290, Nov. 2006.
- [16] P. B. Johnson and R. W. Christy, "Optical constants of the noble metals," *Phys. Rev. B, Condens. Matter*, vol. 6, no. 12, pp. 4370–4379, Dec. 1972.
- [17] P. Sharma and V. D. Kumar, "All optical logic gates using hybrid metal insulator metal plasmonic waveguide," *IEEE Photon. Technol. Lett.*, vol. 30, no. 10, pp. 959–962, May 15, 2018.
- [18] [Online]. Available: <https://refractiveindex.info/>
- [19] A. S. Maier, *Plasmonics: Fundamentals and Applications*. New York, NY, USA: Springer, 2007.
- [20] D. K. Gramotnev and S. I. Bozhevolnyi, "Plasmonics beyond the diffraction limit," *Nature Photon.*, vol. 4, no. 2, pp. 83–91, Jan. 2010.